Int. J. Electrochem. Sci., 13 **(2018)** 3874 – 3887, doi: 10.20964/2018.04.11

International Journal of
ELECTROCHEMICAL
SCIENCE
www.electrochemsci.org

Degradation of a High Build Epoxy Primer/Polyurethane Composite Coatings under Cyclic Wet–dry Conditions

Yuming Tang[1*], *Jingyi Cao*[2], *Shuai Qu*[3], *Le Quan*[1], *Xuhui Zhao*[1], *Yu Zuo*[1]

[1] Beijing Key Laboratory of Electrochemical Process and Technology for Materials,
Beijing University of Chemical Technology, Beijing100029, China;
[2]Navy Coatings Analysis and Detection Centre, Beijing, China;
[3] AVIC BIAM New Materials Technology & Engineering Co., Ltd, Beijing, China
*E-mail: tangym@mail.buct.edu.cn

Received: 27 November 2017 / *Accepted:* 28 December 2017 / *Published:* 6 March 2018

The degradation of a high build epoxy anti-corrosion primer and a grey polyurethane topcoat on carbon steel were investigated under cyclic wet–dry and 3.5% NaCl solution immersion conditions by electrochemical impedance spectroscopy (EIS), Fourier transform infrared spectroscopy (FTIR) and scanning electron microscopy (SEM). The process was compared with that of a composite coat comprising the high build epoxy primer and a polyurethane topcoat. The results show that, under wet–dry conditions, the water absorption was lower than that in the continuous immersion test, but with time, the wet–dry cycles promoted more micropores in the coatings, which accelerated the penetration of the corrosive electrolyte into the coating and thereby caused a barrier performance decrease in the later process. The effect of the cyclic wet–dry conditions on the composite coating was smaller than that on the single-layer coating. The protective properties of the composite coating mainly depended on the high build epoxy anti-corrosion primer.

Keywords: cyclic wet–dry; coating performance; EIS; epoxy primer; polyurethane topcoat

1. INTRODUCTION

Organic coatings are widely used to protect steel structures from corrosion in marine environments. Under most service conditions, such as splash and tidal zones, multilayer organic coatings are often employed to prevent severe corrosion damage under cyclic wet–dry exposure in chloride-containing environments. The degradation process of organic coatings in simulated seawater environments has been frequently studied [1–3], but there has been less focus on the degradation of coatings under cyclic wet–dry conditions [4]. Some previous work [5–8] showed that wet–dry cycles could accelerate the deterioration process of organic coatings. One reason is that cyclic wet–dry conditions may enhance the formation of defect sites in the coatings, and the other explanation is that the repeated wet–dry process may promote delamination of the coating. Györik *et al.* [9] studied the degradation process of styrene–acrylate resin-based water-borne paint coatings and drew a different conclusion, where the wet–dry cycling procedure had a beneficial effect on the protective properties. The authors suspected that this is caused by the dissolution and removal of the water-soluble components of the paint film. Zhang *et al.* [10] investigated the influence of wet–dry cycles and found that compared with immersion, the 4–4 h wet–dry cycles accelerated the coating deterioration, while 12–12 h cycles decelerated the entire deterioration process. Park *et al.* [11] investigated water absorption in four different double-layer coatings, comprising epoxy and urethane layers, under cyclic wet–dry exposure in chloride-containing environments. The results show that water absorption in the coatings is strongly dependent on their constitution and chemical nature.

Based on the aforementioned studies, more coatings need to be studied to further understand the failure process of different organic coatings under various cyclic wet–dry conditions. The high build epoxy anti-corrosion primer is a very good anti-corrosion coating used for marine ships and grey polyurethane heat reflection top paint is widely used in marine atmospheric environments. In this study, the degradation process of a composite coating system, which comprises a high build epoxy anti-corrosion primer and a grey polyurethane topcoat, under wet–dry cyclic conditions was studied. The result was also compared with that of the primer and the topcoat, to help analyze the influence of cyclic wet–dry conditions on the degradation of the composite coating.

2. EXPERIMENTAL

2.1 Materials and Preparation of Samples

The metal substrate was Q235 carbon steel, with the size of 70 mm×150 mm×1 mm. The applied coatings were a bi-component H900 high build epoxy anticorrosive coating and a bi-component SRF2088 polyurethane heat reflection topcoat, produced by Shanghai Haiyue Coating Co., Ltd. (Shanghai, China). The high build epoxy coating was composed of bisphenol A epoxy resin and a tertiary amine curing agent, with aluminum powder, silicon dioxide and iron oxide as pigments. The liquid epoxy was 45%–55% (mass fraction) and pigment 35%–40% (mass fraction). The heat reflection polyurethane topcoat was composed of urethane and hydroxy acrylic resins, with titanium dioxide, dryer, auxiliaries and solvents.

The steel substrate surface was abraded manually with 120# abrasive paper and then cleaned with acetone. The coatings were brushed manually on the substrate and then the coated samples were kept in air for one week at room temperature for complete curing. The dry film thickness of the coating was measured with a TT220 ferromagnetic film thickness tester (Time Instruments Co. Ltd., Beijing, China) at ten random points on the surface and the values were averaged. Table 1 shows the coating systems prepared in this work. 1# coating was a single layer of high build epoxy anticorrosive primer (150 μm). 2# coating was a single layer of polyurethane topcoat (80 μm). The 3# coating system was a two-layer coating comprising high build epoxy anticorrosive primer (150 μm) and polyurethane topcoat (80 μm).

Table 1. Coating systems prepared and their thicknesses.

Number	Primer	Topcoat	Total thickness
1#	high build epoxy (150 μm)	-	150 ± 5 (μm)
2#	-	polyurethane (80 μm)	80 ± 5 (μm)
3#	high build epoxy (150 μm)	polyurethane (80 μm)	230 ± 10 (μm)

2.2 Experimental Conditions

The coated samples were tested, respectively, in the following corrosion environments at room temperature: (i) immersion in 3.5% NaCl solution completely and (ii) in an alternate condition of 4 h immersion in 3.5% NaCl solution and 8 h drying in air. Each cycle was 12 h. This was performed on equipment made by ourselves, in which the cycles were automatically repeated. For each condition, the NaCl solution was replaced once a week.

2.3 Test methods

Electrochemical impedance spectroscopy (EIS) measurements were performed on the coated samples after they were removed from the aforementioned experimental conditions. The test was carried out using a PARSTAT 2273 electrochemical system (Princeton Applied Research, USA) in a 3.5% NaCl solution at room temperature. A section of polyvinyl chloride tube with a 3.7 cm diameter was sealed on the coated sample with the epoxy resin and curing agent, holding the test solution. Thus, the exposed area of the working electrode was 10.7 cm^2. A three-electrode cell was used, in which the reference electrode was a saturated calomel electrode and the counter electrode was a platinum electrode. The measured frequency range was 10^5–10^{-2} Hz and the amplitude of the sinusoidal voltage signal was 10 mV. In each condition, there were at least three parallel samples. ZSimpWin software was used to analyze the EIS spectra to obtain the electrochemical parameters of the coatings.

The coating surface was observed with an optical microscope and a Hitachi S4700 scanning electronic microscope (SEM) (Japan). Changes in the organic functional groups were analyzed with a TENSOR27 infrared spectrometer (Germany). The coating powders removed from the samples were pressed into thin pieces for Fourier transform infrared (FTIR) analysis. The window material was KBr. The spectral resolution was 4 cm^{-1} and the number of scans was 30.

3. RESULTS AND DISCUSSION

3.1 Electrochemical impedance spectroscopy measurements

Figures 1 and 2 show the impedance spectra of the high build epoxy primer coated sample (1#) under cyclic wet–dry and immersion conditions for different times. At the beginning, the Bode plot under each condition shows typical capacitive behavior, characterized by a straight line with a slope of −1 and a $|Z|_{0.01Hz}$ (impedance magnitude at 0.01 Hz frequency) value of ~10^{11} Ω cm^2, indicating very good barrier properties of the coating to the substrate [12]. The impedance then decreased over time. Under wet–dry conditions, from 199 d, the spectra began to demonstrate two time constants, and an impedance plateau was observed in the low frequency region in the Bode plot, indicating that the electrolyte may have reached the coating/metal interface and the corrosion process may have occurred on the metallic substrate [13]. In the whole cyclic wet–dry process, the $|Z|_{0.01Hz}$ value of the sample decreased by three orders of magnitude. However, under immersion conditions, the $|Z|_{0.01Hz}$ value only dropped by one and a half orders of magnitude, without an apparent second time constant shown in the Nyquist plot, demonstrating that the good barrier properties remained.

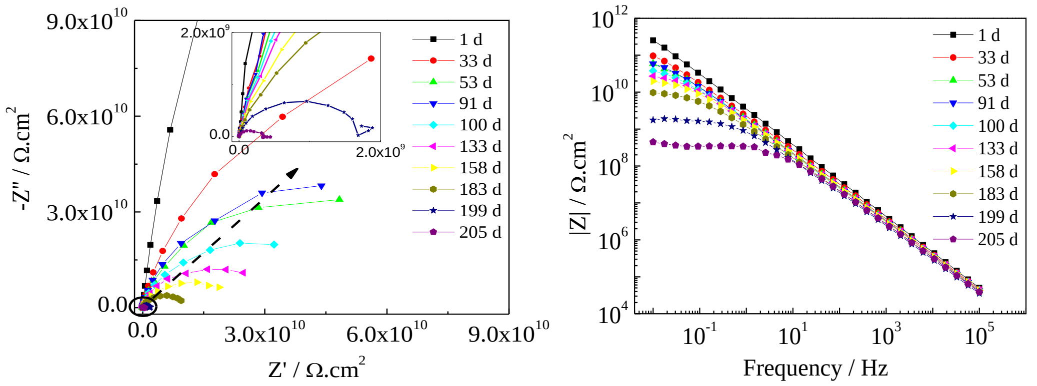

(a) Nyquist (b) Bode

Figure 1. Impedance spectra of the epoxy primer sample (1#) after wet–dry testing for 205 d.

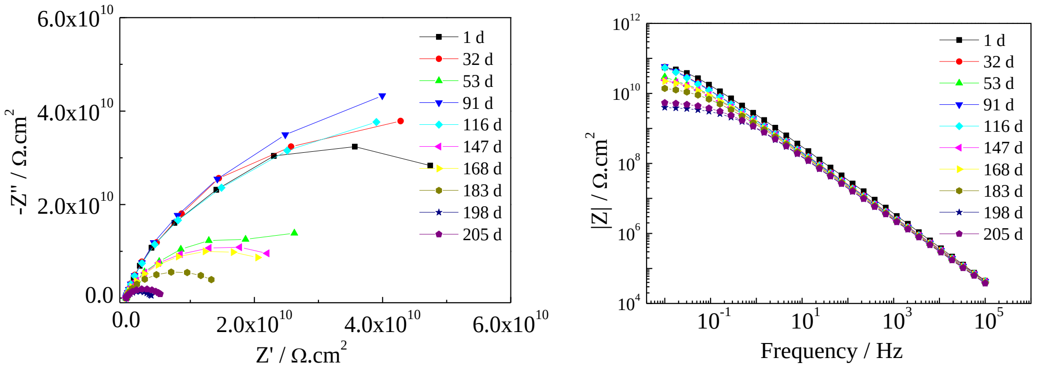

(a) Nyquist (b) Bode

Figure 2. Impedance spectra of the epoxy primer sample (1#) after immersion for 205 d.

Figures 3 and 4 show the EIS spectra of the polyurethane topcoat coated sample (2#) under cyclic wet–dry and immersion conditions. Compared with the epoxy primer sample, the initial $|Z|_{0.01Hz}$ values of the polyurethane topcoat sample under the two conditions were comparatively lower at ~1×10^{10} Ω cm^2. With time, the impedance under cyclic wet–dry conditions dropped quickly. After 183 d, an impedance plateau appeared in the low and middle frequency range, indicating that the electrolyte had penetrated through the coating to the metal surface and the corrosion reaction started to occur [13]. Over time, the impedance plateau at low frequency became more obvious and moved towards the intermediate frequency region. Figure 4 shows that the decrease rate of the impedance under immersion conditions was comparatively slow. At 205 d, the $|Z|_{0.01Hz}$ value was $5×10^8$ Ω cm^2, which was one order higher than that for the cyclic wet–dry test ($8.5×10^7$ Ω cm^2).

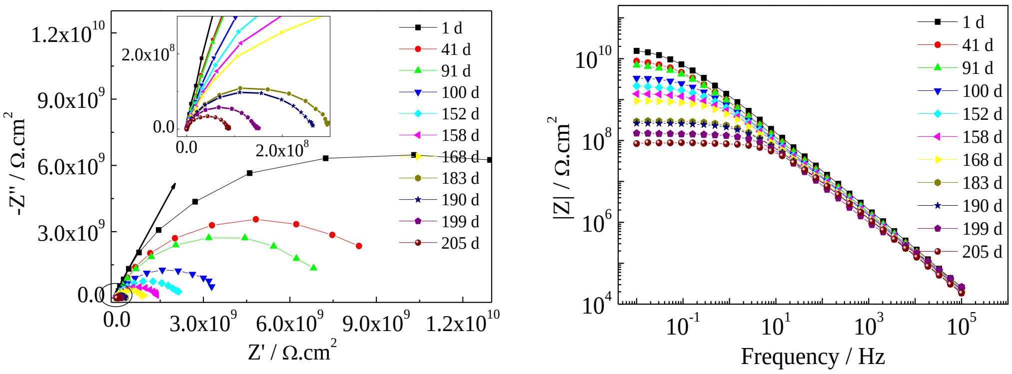

(a) Nyquist (b) Bode

Figure 3. Impedance spectra of the polyurethane topcoat (2#) after wet–dry test for 205 d.

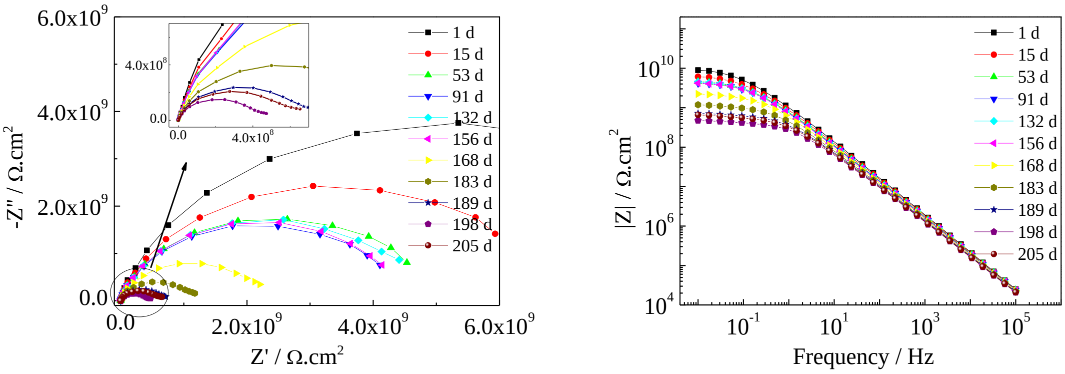

(a) Nyquist (b) Bode

Figure 4. Impedance spectra of the polyurethane topcoat (2#) after immersion for 205 d.

Figures 5 and 6 show the impedance spectra of the two-layer composite coating sample (3#) under two conditions. At the beginning, the plot presented typical capacitive behavior with high impedance ($|Z|_{0.01Hz}$ value higher than $1×10^{11}$ Ω cm^2) under each condition. After 205 d, there was still no clear second time constant shown under both conditions and the value of $|Z|_{0.01Hz}$ was higher than 10^9 and 10^{10} Ω cm^2, respectively. Thus, the coatings still had very good barrier properties [12,13]. During the testing process, the $|Z|_{0.01Hz}$ impedance of the sample exposed to the wet–dry environment dropped by two orders of magnitude, while that under immersion conditions only dropped by less than one order of magnitude.

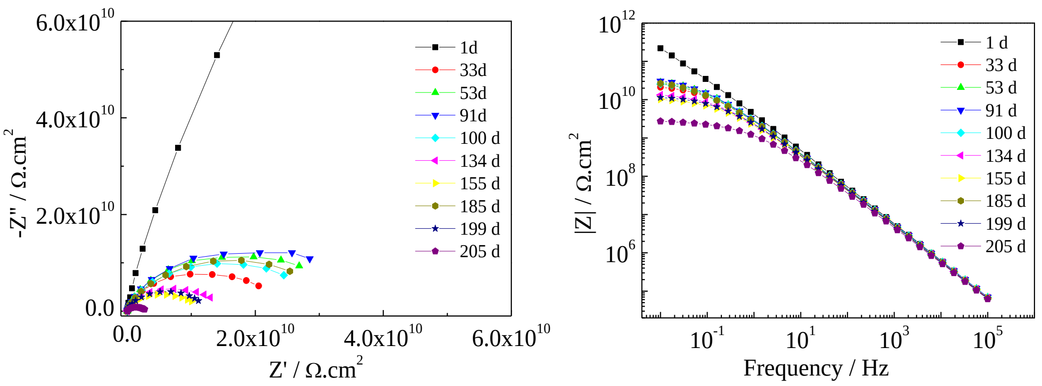

(a) Nyquist (b) Bode

Figure 5. Impedance spectra of the composite coating sample (3#) after wet–dry test for 205 d.

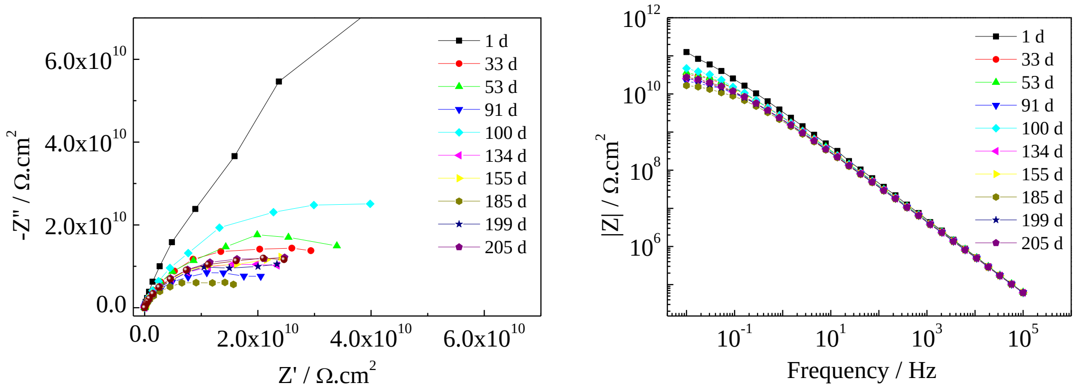

(a) Nyquist (b) Bode

Figure 6. Impedance spectra of the composite coating sample (3#) after immersion for 205 d.

Figure 7 shows $|Z|_{0.01Hz}$ variations of the three coating samples versus testing time. During the early period (170 d for 1# and 140 d for 2#), the $|Z|_{0.01Hz}$ values of both the epoxy (1#) and polyurethane coatings (2#) under wet–dry cycle testing were higher than those under immersion (Figure 7(a)), but then the impedance under wet–dry conditions began to decrease rapidly and became lower than that in the continuous immersion. Thus, compared with the immersion conditions, the wet–dry cycling had less of a negative effect on the barrier properties during the early period and an obvious negative effect in the later process for the two single-layer coatings. This was consistent with the previous result [10], where the authors studied the deterioration process of an iron oxide red alkyd primer and noted that, compared with the immersion process, wet–dry cycles resulted in higher impedance during the early stage, which was termed as the medium penetration stage, before steel corrosion occurred. In Figure 7(b), for the composite coating (3#), before 180 d, the impedance under two conditions showed no significant difference. After 180 d, the impedance under wet–dry cycling conditions began to decrease rapidly, while the impedance under the immersion test still retained a high value. This indicates that the cyclic wet–dry conditions had no apparent effect on the early stage, but caused an impedance decrease in the later process of the composite coating. Compared with the one-layer coatings and the two-layer composite coating, it can be found that the wet–dry cycling had a similar effect on the impendence variation of the epoxy primer, polyurethane topcoat and composite coating system. However, the composite coating system presented better protective properties and its impedance value is relatively close to that of the high build epoxy primer, demonstrating that the protective properties of the composite coating mainly depended on the high build epoxy anti-corrosion primer.

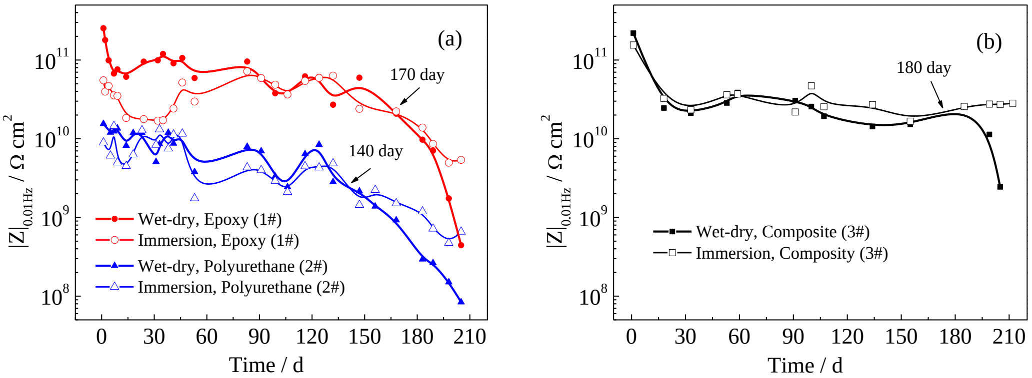

Figure 7. $|Z|_{0.01\mathrm{Hz}}$ values after tests exposed to wet–dry and immersed environments for (a) samples 1# and 2# and (b) 3#.

3.2 The water absorption and porosity of three coatings under two conditions

By fitting an equivalent circuit to the EIS data, the values of the equivalent circuit elements were obtained. Figure 8 shows the equivalent circuit models, in which R_s is the electrolyte resistance, R_{po} is the coating resistance, Q_c is a constant phase element replacing the coating capacitance (C_c), and R_{ct} and C_{dl} correspond to the charge transfer resistance and double layer capacitance at the coating-metal interface, respectively. When n equals 1, Q_c simplifies to a capacitance C_c, and when n = 0, Q_c simplifies to a pure resister. Model A was used to fit the EIS data for 3# under two conditions, 1# and 2# under immersion conditions and 1# and 2# exposure to the wet–dry environment before 183 and 199 d, respectively. Model B was used for 1# and 2# under wet–dry conditions after 183 and 199 d, respectively.

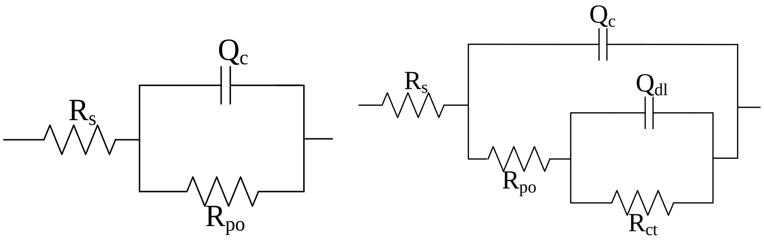

(a) Model A (b) Model B

Figure 8. Equivalent circuit models.

The water volume fraction (φ) in the coating was calculated from the coating capacitance using Eq. (1) [1,14,15], where C_t is the coating capacitance at time t, C_0 is the initial coating capacitance, ε_w

is the relative permittivity of water at 25 °C (80). The coating capacitance (C_c) can be calculated using Eq. (2) [15–17], where Q_c, n, R_s and R_{po} are modelling elements for the equivalent circuit. The porosity (P) of the coating can be determined as the ratio of the theoretical bulk resistance of the coating at 'infinite' porosity (R_e) to the measured coating bulk resistance (R_{po}) (see Eq. (3)) [18], where R_e was calculated by Eq. (4), d represents the coating thickness (μm), A represents the electrode area (cm^2), k is the conductivity of the electrolyte (0.01 S·m^{-1}, 3.5% NaCl, 25 °C) and R_{po} is the measured coating bulk resistance (Ω cm^2).

$$\phi = \frac{\log(C_t / C_0)}{\log \varepsilon_w} \tag{1}$$

$$C_c = Q_c^{1/n}(R_s^{-1} + R_{po}^{-1})^{(n-1)/n} \tag{2}$$

$$P = (R_e) / R_{po} \tag{3}$$

$$R_e = d / Ak \tag{4}$$

Figure 9 shows the water volume fraction (*φ*, %) values of the three coatings versus testing time. For the epoxy primer (1#) and composite coating (3#), the water uptake under wet–dry cyclic testing was lower than that under continuous immersion testing. The probable explanation was that the water absorption of the organic coatings is comparatively slow, while the water desorption is faster, which might be because the swelling of the paint resin during water penetrating could hinder the entering of additional water into the interior of the paint, and during the dry period, the polymer particles shrink, thereby facilitating water release from the interior towards the interface [9]. The polyurethane topcoat (2#) presents a higher water volume fraction, and it seems there is no obvious difference between the water volume fraction under the two conditions. This was probably because the thickness of the polyurethane topcoat is thinner, so that water can pass through the layer more easily in the wet stage, then the dry stage has less influence on the water uptake volume. The epoxy primer (1#) presents a much lower water volume fraction, demonstrating that the high build epoxy coating had good water resistance. It also can be seen that the value of water volume fraction in the two-layer coating (3#) is similar to that in the high build epoxy primer, presenting a lower value. This demonstrates that the composite coating blocked the ingress of water into the coating effectively, and the high build epoxy primer played a major role in the water resisting process.

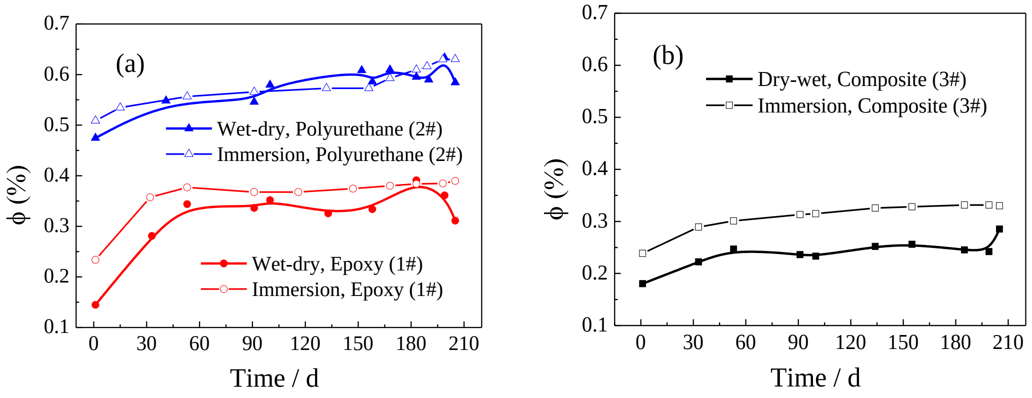

Figure 9. Water volume fraction (*φ*) under the two conditions for (a) samples 1# and 2# and (b) 3#.

Compared with the capacitance, the resistance is more sensitive to the presence of micropores, defects or heterogeneities in the coatings [19]. The porosity (*P*) of the coatings calculated by the coating resistance is shown in Figure 10. It is seen that the porosity of the high build epoxy primer (1#) is much lower than that of the polyurethane topcoat (2#). However, for all coatings, during the early stage, the porosity of the coating under wet–dry cycling was lower than that under immersion, but with time, it increased faster. This might be because after exposure to the cyclic wet–dry environment, the fast water desorption and slow water absorption processes led to a lower water absorption volume in the coating (Figure 9). Consequently a larger coating resistance compared to that under immersion conditions was obtained [7], and thus a lower coating porosity was calculated by Eq. (2). As the cyclic wet–dry test continued, the coating experienced repeated swelling/shrinking due to the water adsorption/desorption process [7,10], which could lead to an increase in the number and size of the micropores, local defects and heterogeneities in the coatings. The penetration of the corrosive media, such as water, oxygen and Cl^- ions, through the coating was accelerated and the porosity in the coating was facilitated. The results in Figures 7, 9 and 10 show that though the wet–dry cyclic conditions had a negative effect on the water adsorption of the coatings, causing a lower water volume fraction, which promoted the porosity in the coatings after some cycles and could supply more transport pathways for the corrosive media penetrating through the coating. This causes the barrier performance of the coating to decrease. It also can be seen that for most of the test time, the porosity of the composite coating was higher than the one-layer epoxy primer, this is because the composite coating comprised epoxy primer with low porosity and polyurethane top coat with high porosity. However, probably due to its larger coating thickness, it would take a longer time for the wet–dry cycle to facilitate the micropores or local defects in the deeper paint of the composite coating.

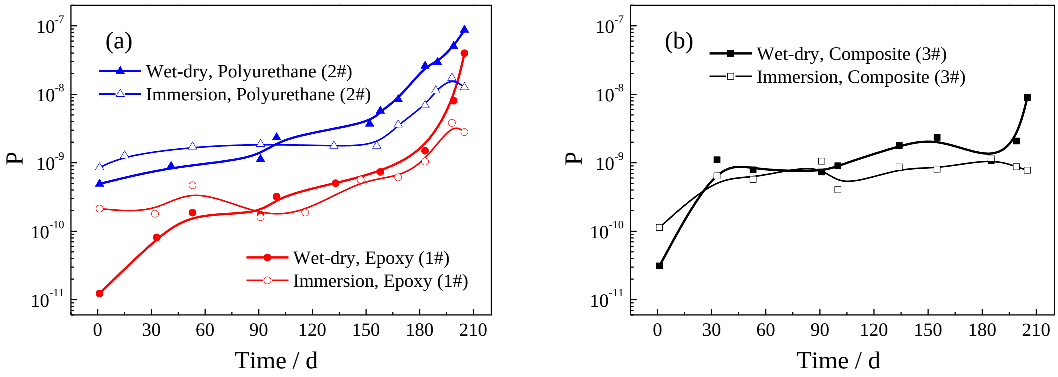

Figure 10. Porosity (*P*) under the two conditions for (a) samples 1# and 2# and (b) 3#.

3.3 The FTIR result and SEM morphology of the coatings under two conditions

Figure 11 shows the infrared spectra of the epoxy primer (1#) and the polyurethane topcoat (2#) after 205 d under two experimental conditions, which are compared with the spectra before exposure. The main wavenumbers used to characterize the degradation of the coatings are depicted in Table 2 [7,20–29]. To make comparison of the individual peaks of interests, before and after the test, all spectra were normalized using the C–H stretching vibration of CH_2 groups at 2923 cm^{-1} [23,24]. In Figure 11(a), after the 205 d test, the intensity of the -OH (3427 cm^{-1}) band increased obviously, indicating that some new hydroxyl function groups had formed. This was probably caused by the uptake of water into the coating and/or the occurrence of hydrolytic degradation of the coating [20,24]. The reduction of the C–O–C (1246 cm^{-1}) and C–N (1029 cm^{-1}) bands can both be assigned to the degradation of the epoxy coating [20]. In Figure 11(b), the large increase in the -OH (3427 cm^{-1}) band intensity also indicates the hydrolytic degradation of the polyurethane coating. The disappearance of C–O stretching at 1145 cm^{-1} and the decreased intensity of –COO (1447 cm^{-1}) and C=O (1727 cm^{-1}) bands demonstrate the reduction of polyurethane components [7,23,25]. For both the epoxy primer and polyurethane topcoat, the wet–dry cycling led to a more apparent chemical changes of the coatings, which was consistent with the lower impedance and higher porosity results shown earlier..

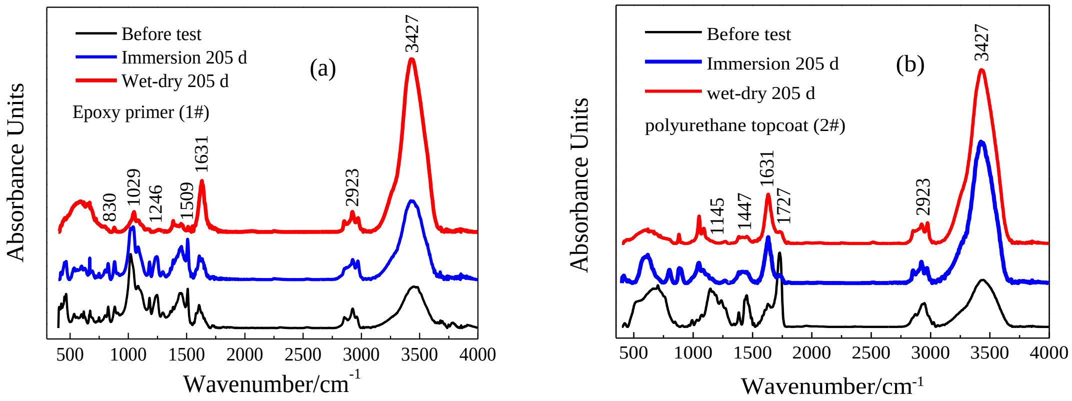

Figure 11. FTIR spectra of (a) 1# and (b) 2# coatings after the 205 d test under two conditions.

Table 2. IR band assignments for the primer and topcoat.

Wavenumber (cm^{-1})	Assignment	Literature
3427	hydroxyl (O-H)	[20,21,24,28]
2923	methylene (-CH_2)	[7,21,22,24,26]
1727	C=O in esters	[7,21–23,26]
1631	N–H in primary amine	[20]
1447	-COO	[7,23]
1246	etheric band (C–O–C)	[7,20,22,23]
1145	C–O in ester	[25,27,29]
1029	C–N in urethane	[20]

Figure 12 shows the IR spectra of the composite coating (3#) after the 205 d test under two conditions, compared with the spectra of the epoxy primer (1#) and the polyurethane topcoat (2#) before the test. There was no large difference in the chemical changes for the composite coating under two conditions, both the topcoat and primer in the composite coating presented hydrolytic degradation. This is consistent with the results in the EIS test, which is the composite coating under two conditions, showing high impedance (higher than 1×10^9 Ω cm^2) without an obvious difference during the test.

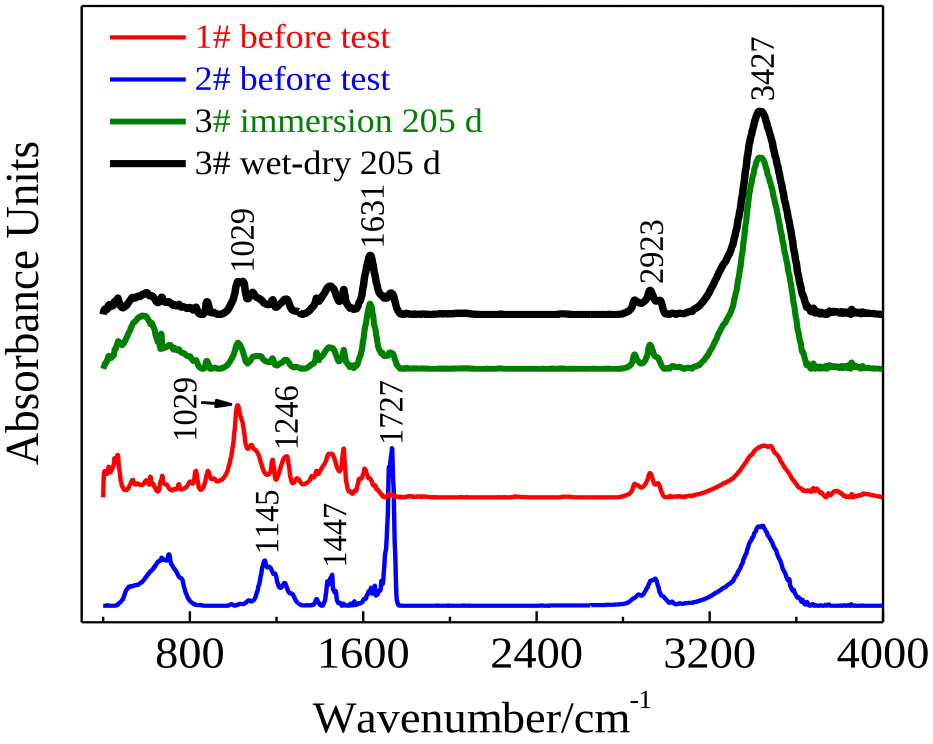

Figure 12. FTIR spectra of composite coating (3#) after 205 d test under two conditions.

Figure 13 shows the SEM images of the composite coating after the 119 and 205 d tests under two conditions, respectively. Before the test, the coating presented a flat and intact surface. After the test, some cracks and micropores were evident on the surface, which were probably caused by the physical damage from water absorption and the hydrolytic degradation of the coating. With time extended, more micropores were observed, which developed deep into the coating. After 205 d, it seemed that the micropores on the coating surface under wet–dry conditions were deeper than those under immersion conditions. This indicates that the repeated swelling/shrinking due to the water adsorption/desorption process had an accelerating effect on the development of the micropores after a certain period. From the FTIR spectra, at this time, severe hydrolytic degradation already occurred in the primer coating. This indicates that the micropores formed in the topcoat might penetrate deep into the primer and the barrier performance of the topcoat against corrosive electrolyte diffusion decreased. The results of SEM and FTIR were consistent with the coating porosity results from EIS data.

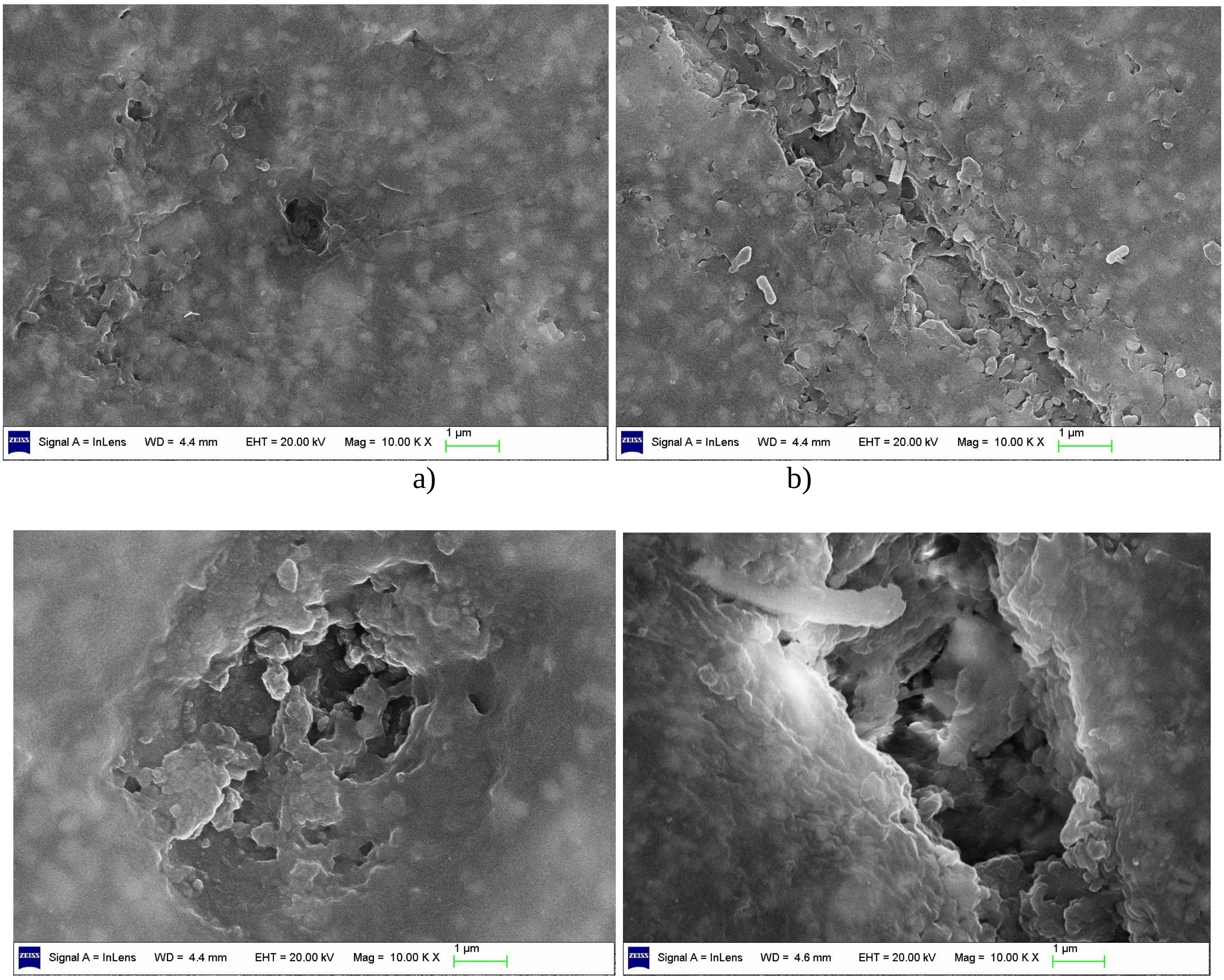

a) b)

c) d)

Figure 13. SEM morphologies of the composite coating surface after tests: a), c) immersion tests for 119 and 205 d; b), d) wet–dry tests for 119 and 205 d.

The foregoing results show that for the high build epoxy anti-corrosion primer and the polyurethane topcoat single-layer coating, compared with the immersion test, the coating performance under the wet–dry conditions decreased slowly in the early process and more quickly in the later process. This is different from the results in the literature [10], compared with immersion, the 4–4 h wet–dry cycles accelerated the deterioration of the coating (iron oxide red alkyd primer), but the 12–12 h cycles decelerated the entire deterioration process. These authors thought that this was because during the long drying process in the 12–12 h wet–dry cycles, the penetrated water can be exhausted completely. In this study, the alternate condition was 4 h immersion in 3.5% NaCl solution and 8 h drying in air. The cyclic ratio was lower than that of the 4–4 h cycles and higher than the 12–12 h cycles. The reason for the relatively slower decrease in coating performance in the early process could be explained by the decreased water adsorption of the coatings in the wet–dry cyclic procedure, in which the water uptake is slow and the release is fast [9]. The lower water adsorption resulted in a higher impedance of the coatings. As the cyclic wet–dry test continued, the coating experienced repeated swelling/shrinking in the water adsorption/desorption process, which increased micropores and defects in the coatings and promoted the hydrolytic degradation of the coating. More micropores and defects could supply more transport pathways for the corrosive media to penetrate into the coating, causing the barrier performance of the coating to decrease. As it takes time for the repeated swelling/shrinking in the water adsorption/desorption process to increase the porosity in the coatings, the wet–dry cycles mainly accelerated the later period of the deterioration process. The composite coating (the high build epoxy primer/polyurethane topcoat) was thicker and had better barrier properties, so it would take a longer time to observe the accelerating effect of the wet–dry cycling on the degradation of the coating system.

In addition, because the water absorption capability of coatings was strongly dependent on the chemical and physical natures of the materials, the wet–dry cycles may have different effects on different coating systems [9,11]. A further study will be carried out to understand the failure process of more organic coatings under wet–dry cycling.

4. CONCLUSIONS

The cyclic wet–dry conditions had no apparent effect on the early stage, but caused an impedance decrease in the later process of the composite coating. The protective property of the composite coating mainly depended on the high build epoxy anti-corrosion primer, which played a major role in the water resisting process.

The wet–dry cycling had a negative effect on the water adsorption of the coatings, causing a lower water volume fraction, but after many cycles, the micropores in the coatings were promoted, which could supply more transport pathways for the corrosive media penetrating through the coating and caused the barrier performance to decrease.

References

1. S.P. He, J.P. Xiong, Y.M. Tang and Y. Zuo, *Electrochem.*, 16 (2010) 362. [In Chinese]
2. W. Shi and S.B. Lyon, *Prog. Org. Coatings*, 102 (2017) 66.
3. R. Pang, Y. Zuo, Y.M. Tang and J.P. Xiong, *Acta Phys.-Chim. Sin.*, 28 (2012) 1146.
4. S.B. Lyon, R. Bingham and D.J. Mills, *Prog. Org. Coatings*, 102 (2017) 2.
5. W. Zhang, J. Wang, Z.Y. Zhao and X.Q. Liu, *J. Chin. Soc. Corros. Prot.*, 31 (2011) 329. [In Chinese]
6. L. Zhang, Y. M. Tang and Y. Zuo, *J. Chem. Ind. Eng.*, 62 (2011) 1977. [In Chinese]
7. M. Hattori, A. Nishikata and T. Tsuru, *Corros. Sci.*, 52 (2010) 2080.
8. D. Zhang, H. Qian, L. Wang and X. Li, *Corros. Sci.*, 103 (2016) 230.
9. G. Lendvay-Györik, T. Pajkossy and B. Lengyel, *Prog. Org. Coatings*, 56 (2006) 304.
10. W. Zhang, X.Z. Chen, P.F. Yin, Z.K. Xu, B. Han and J. Wang, *Appl. Mech. Mater.*, 161 (2012) 58.
11. J.H. Park, G.D. Lee, H. Ooshige, A. Nishikata and T. Tsuru, *Corros. Sci.*, 45 (2003) 1881.
12. J.M. McIntyre and H.Q. Pham, *Prog. Org. Coatings*, 27 (1996) 201.
13. Z. Feng and G.S. Frankel, *Electrochim. Acta*, 187 (2016) 605.
14. L.V.S. Philippe and S.B. Lyon, C. Sammon and J. Yarwood, *Corros. Sci.*, 50 (2008) 887.
15. Q. Zhou and Y. Wang, *Prog. Org. Coatings*, 76 (2013) 1674.
16. S.P. Harrington and T.M. Devine, *J. Electrochem. Soc.*, 156 (2009) C154.
17. N. Fredj, S. Cohendoz, X. Feaugas and S. Touzain, *Prog. Org. Coatings*, 74 (2012) 391.
18. R.D. Armstrong, A.T.A. Jenkins and B.W. Johnson, *Corros. Sci.*, 37 (1995) 1615.

19. M.D.G. Destreri, J. Vogelsang, L. Redrizzi and F. Deflorian, *Prog. Org. Coatings*, 37 (1999) 69.
20. E. Matin, M.M. Attar and B. Ramezanzadeh, *Prog. Org. Coatings*, 78 (2015) 395.
21. A. Colin, M. Baba, P.O. Bussiere, E. Cavaletti, F. Nizeyimana and S. Therias, *Polym. Degradation Stab*., 114 (2015) 115.
22. F.X. Perrin, M. Irigoyern, E. Aragon and J.L.Vernet, *Polym. Degradation Stab*., 72 (2001) 115.
23. X.F. Yang, C. Vang, D.E. Tallman, G.P. Beirwagen, S.G. Croll and S. Rohlik, *Polym. Degradation Stab*., 74 (2001) 341.
24. F.X. Perrin, C. Merlatti, E. Aragon and A. Margaillan, *Prog. Org. Coatings*, 64 (2009) 466.
25. F. X. Perrin, M. Irigoyen, E. Aragon and J.L. Vernet, *Polym. Degradation Stab*., 70 (2000) 469.
26. C. Merlatti, F.X. Perrin, E. Aragon and A. Margaillan, *Polym. Degradation Stab*., 93 (2008) 896.
27. K. Karadeniz, Y. Calikoglu, and M.Y. Sen, *Polym. Bull*., 74 (2017) 2819.
28. V. Mishra, J. Desai and K.I. Patel, *Ind. Corp. Prod.*, 111(2018) 165.

29 F. Yang, L. Zhu, D. Han, R. Cao, W. Li, Y. Chen, X. Wang and L. Ning, *Prog. Org. Coatings*, 90 (2016) 455.